JOC Article

Chiral Aromaticities. AIM and ELF Critical Point and NICS Magnetic Analyses of Möbius-Type Aromaticity and Homoaromaticity in Lemniscular Annulenes and Hexaphyrins
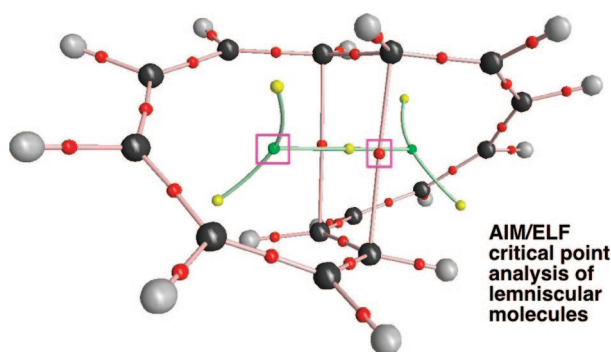
Charlotte S. M. Allan and Henry S. Rzepa*

Department of Chemistry, Imperial College London, South Kensington Campus, London SW7 2AZ, U.K.

rzepa@ic.ac.uk

Ⓦ **This paper contains enhanced objects available on the Internet at http://pubs.acs.org/joc.**

AIM/ELF critical point analysis of lemniscular molecules

An atoms-in-molecules (AIM) and electron localization function (ELF) critical point analysis is reported for two types of lemniscular system, each of which exhibits double-half-twist Möbius topology. This reveals that this type of conformation for [14]annulene **1** has, in addition to the obvious bond critical points (BCPs), two weaker transannular points in the central cross-over region. These can be interpreted in terms of local rings showing single-half-twist Möbius homoaromaticity in addition to the double-half-twist aromaticity revealed by the annulene as a whole. Another example of a single-half-twist Möbius homoaromatic **9** is suggested here to show aromatic properties as strong as its nonhomoaromatic analogue **8**. The AIM critical points in **1** are relatively insensitive to the ring size (varied from 12 to 16), and only small changes are seen in the critical point properties when the π-electron count is incremented from 4n+2 to 4n by dianion formation. These results are discussed in terms of the reported transformation of the 14-π-electron octalene **10** by reduction/alkylation into **12**, an isomer of **1**. Another class of molecule that exhibits lemniscular topology is the phyrins. A transannular BCP in the central cross-over region for the double-half-twist aromatic [26]hexaphyrin **3** is revealed, which is not present for the double-half-twist antiaromatic [28]hexaphyrin **2**. The NICS(rcp) for the former indicates strong Möbius homoaromaticity.

It has recently been recognized[1] that *figure-eight* shaped conjugated annulenes are examples of double-twisted Möbius cycles, an extension of the single-twisted category first suggested by Heilbronner in 1964.[2] Such figure-eight, or *lemniscular*, character exhibits a topological property known as writhe, a property also exhibited by cyclic DNA oligomers.[3] We have

recently shown[4] that writhe represents a mechanism for converting overlap-reducing local twists of adjacent 2p atomic orbitals in a π-conjugated annulene into bending distortions in 3D space and that this phenomenon may account for the surprisingly relative stability (with respect to untwisted forms) of this form of molecule. One particular annulene, the D_2-symmetric 14π-electron **1** was calculated[1] to be entirely π-delocalized and aromatic. This was assessed by the (predicted) lack of bond length alternation around the ring (Δ_r, the difference between

(1) (a) Rzepa, H. S. *Org. Lett.* **2005**, *7*, 4637–4639. (b) Rzepa, H. S. *Chem. Commun.* **2005**, 5220–5222.
(2) Heilbronner, E. *Tetrahedron Lett.* **1964**, 1923–1928.
(3) Rossetto, V.; Maggs, A. C. *J. Chem. Phys.* **2003**, *118*, 9864–9874.

(4) Rappaport, S.; Rzepa, H. S. *J. Am. Chem. Soc.* **2008**, *130*, 7613–7619.

longest and shortest C−C bond in the cycle, was <0.01 Å for this system) and the negative nucleus-independent chemical shift (NICS) value[5] at the ring centroid, indicative of a prominent diamagnetic ring current. Such a coiled helical annulene also has another feature not found in uncoiled systems, namely, at the cross over point of the lemniscate, a local π–π self-stacking arrangement occurs. The annulene **1** also has some parallel in the recently reported[6] [28]hexaphyrin **2** and [26]hexaphyrins **3**. Like **1**, these too adopt a lemniscular conformation (characterized in this case by crystal structures), and while the former is a 4n electron antiaromatic species, the [26]phyrin is a 4n+2 electron aromatic system. Here, Bader's AIM (atoms-in-molecules) electron density[7] and the related ELF (electron localization function)[8] analyses are used to probe the consequences of the (enforced) π–π stacking in these molecules at the cross-over point of the lemniscate.
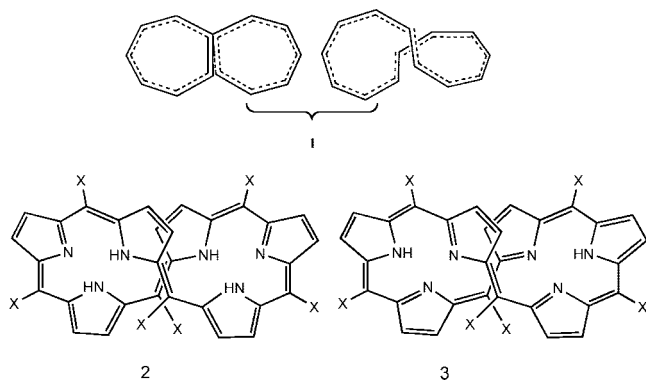
Topological Electronic Analyses

Comprehensive reviews provide an overview of the two principle quantum topological approaches, AIM and ELF,[7] and in particular their application to the analysis of electron delocalization in aromatic molecules.[7a] It is noteworthy that such analyses have traditionally concentrated on planar (Hückel) systems in which σ/π separation is possible, with very much less attention given to helical (Möbius) systems (where strict σ/π separation is not possible).

AIM Analysis.[7] The AIM procedure introduced by Bader[7b] involves analyzing the total electron density by inspection of topological features known as critical points, at which the gradient of the electron density, ρ, vanishes. There are four types of critical points, which differ in the local curvature of the electron density, being distinguished by the signs of the eigenvalues of the corresponding electron density Hessian matrix:

1. A point for which all three matrix eigenvalues are negative corresponds to an **attractor** and essentially coincides with the nuclear positions.
2. Two negative eigenvalues only corresponds to a bond critical point (BCP). The value of the electron density ρ at this point can be approximately interpreted as the strength of interaction between the two adjacent attractors.
3. One negative eigenvalue corresponds to a ring critical point (RCP).
4. All positive eigenvalues corresponds to a cage critical point (CCP).

ELF Analysis.[8] The ELF (electron localization function, $\eta(r)$) was originally proposed by Becke and Edgecombe.[8a] It was extended for use with DFT calculations by Savin et al.[8b] This formulation is related to the excess electron kinetic energy due to Pauli repulsion. As the ELF function tends to 1, electrons are more localized relative to electrons in a uniform electron gas of the same density. When ELF is close to 0.5 the effect of Pauli repulsion approaches that of a uniform electron gas of the same density. Thus ELF provides information relating to localized electron pairs and therefore gives a direct insight into chemical bonding. As with AIM, the ELF function can be used instead of electron density to locate critical points. A volume of space enclosed by a particular ELF isosurface is termed a localization domain. These localization domains may be attractors (denoting nuclei) or basins. Basins may be either core (containing a single nucleus (except H)); valence bonding (between two or more core basins); or nonbonding. Basins are labeled C(X) for core and V(X,X,...) for valence, where X denotes the atom types. A localization reduction diagram (bifurcation tree)[8c–e] describes the evolution of localization domains as ELF is varied from 0 to 1 (Figure 2).

NICS Analysis. The ring and cage points have further relevance to a putatively aromatic system. Schleyer introduced[5] the concept of a nucleus-independent chemical shift (NICS) as an estimate of the nature of the (diatropic or paratropic) ring current in a cyclic conjugated molecule and originally placed this probe at the ring centroid (the NICS(0) value). Because ring currents can originate from electrons of both σ- and π-symmetry, increasingly sophisticated procedures were adopted to try to partition the contributions from these two. These methods work well for systems where a plane of symmetry can define the difference between σ- and π-symmetry, but they are less unique for helical systems where only axes of symmetry can be formally defined, and where ring centroids are more arbitrarily defined if nuclear positions alone are used. In this context, the RCPs and CCPs provide more unique coordinates for estimating the NICS values for such helical systems; these are termed NICS(rcp) or NICS(ccp) here. A review of NICS compared to other local aromaticity indices has recently appeared,[5c] although again with the focus on planar rather than helical (nonplanar) systems.

Computational Procedures

The B3LYP density functional procedure was used with a 6-31G(d) basis (with selected points studied at the aug-cc-pvtz basis set level), as implemented in the Gaussian 03 (revision E.01) program.[9] Five permutations on a [14] 4n+2-electron annulene were selected to study variation in ring size, ranging from the d_2-symmetric dianion of the [12]annulene to the dication of the

(5) (a) Schleyer, P. v. R.; Maerker, C.; Dransfeld, A.; Jiao, H.; van Eikema Hommes, N. J. R. *J. Am. Chem. Soc.* **1996**, *118*, 6317–6318. (b) Chen, Z.; Wannere, C. S.; Corminboeuf, C.; Puchta, R.; Schleyer, P.v. R. *Chem. Rev.* **2005**, *105*, 3842–3888. (c) For a comparison of NICS indices with a range of others, see: Bultinck, P. *Faraday Discuss.* **2007**, *135*, 347–365.

(6) Shimizu, S.; Aratani, N.; Osuka, A. *Chem. Eur. J.* **2006**, *12*, 4909–4918.

(7) (a) Poater, J.; Duran, M.; Sola, M.; Silvi, B. *Chem. Rev.* **2005**, *105*, 3911–3947. (b) Bader, R. F. W. *Atoms in Molecules: a Quantum Theory*; Oxford University Press: Oxford, U.K.; 1990. (c) Popelier, P. L. A. *Atoms in Molecules: an Introduction*; Prentice-Hall: London, 2000.

(8) (a) Becke, A. D.; Edgecombe, K. E. *J. Chem. Phys.* **1990**, *92*, 5397–5403. (b) Savin, A.; Jepsen, O.; Flad, J.; Andersen, O. K.; Preuss, H.; von Schnering, H. G. *Angew. Chem., Int. Ed. Engl.* **1992**, *31*, 187–188. (c) Savin, A.; Silvi, B.; Colonna, F. *Can. J. Chem.* **1996**, *74*, 1088–1096. (d) Calatayud, M.; Andres, J.; Beltran, A.; Silvi, B. *Theor. Chem. Acc.* **2001**, *105*, 299–308. (e) Kohout, M.; Wagner, F. R.; Grin, Y. *Theor. Chem. Acc.* **2002**, *108*, 150–156. (f) Cioslowski, J.; Matito, E.; Sola, M. *J. Phys. Chem. A* **2007**, *111*, 6521–6525.

(9) Frisch, M. J. et al. *Gaussian 03, Revision E.01*; Gaussian, Inc.: Wallingford CT, 2007.
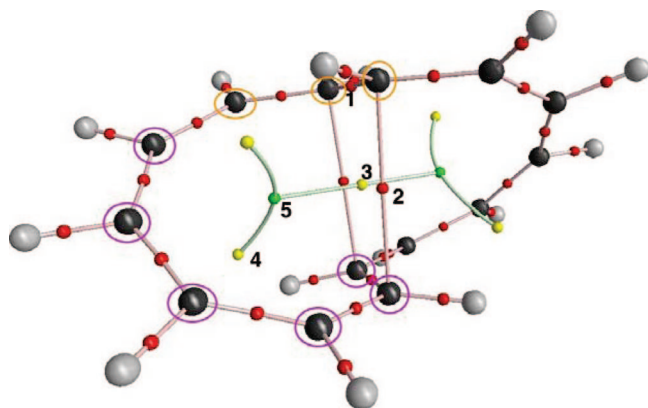
FIGURE 1. Critical points for **1** (BCPs are shown in red, RCPs in yellow, and CCPs in green). The $\rho(r)$ values (in e Å^{-3}, for method B3LYP/6-31G(d) [M05/6-31G(d)] {B3LYP/aug-cc-pvtz}) at points 1−5 are 0.309 [0.304]{0.320}, 0.0193 [0.0211]{0.0225}, 0.0166 [0.0181] {0.0209}, 0.0055 [0.0056] {0.0060}, and 0.0043 [0.0043] {0.0046}, respectively.

[16]annulene. A 4n, 16-electron system was modeled by the dianion of **1**. Two hexaphyrins, a C_2-symmetric [28] 4n-electron form **2** and its oxidized [26] 4n+2 electron form **3** are also included. Transition states were located and characterized via calculation of the Hessian matrix of second derivatives. Biradical-like points were located using the UHF procedure and the Gaussian keyword guess(mix). AIM critical points and the molecular graphs that map their connectivity were obtained by exporting a WFN file from Gaussian and importing into AIM2000[10a] or AIMALL.[10b] The two programs normally give congruent results for critical points, although it was found the latter gave more reliable convergence for bond paths in the molecular graph connecting these points. ELF surfaces were calculated with Dgrid[11] and visualized with VMD[12] using a FCHK file exported from Gaussian. In one case, the ELF surface was calculated using Dgrid and specifying only the (approximately) π-MOs for its evaluation.

Results and Discussion

AIM and ELF Analysis of 1. The AIM critical point analysis for the [14]annulene **1** reveals 28 attractors and 30 BCPs. Of the latter, 28 had $\rho(r)$ values typical of a covalent bond (e.g., point 1, Figure 1), and two showed smaller values (points 2, Figure 1). Five RCPs (points 3, 4) and two CCPs (point 5) complete the analysis, which also fulfills the Poincaré−Hopf condition (attractors − BCP + RCP − CCP = 1). The two additional BCPs (points 2) occur in the lemniscate cross-over region and correspond to a localized 4-carbon $\pi-\pi$ stacking, with C−C distances of 2.734 Å. The $\rho(r)$ value is 0.019 au for each, which is a relatively large value for π-stacking. This density can be related to a stabilizing interaction energy, estimated as −6.6 kcal/mol for **1** from the two BCPs, using the simple relationship given by Platts between the electron density values for BCPs and intermolecular $\pi-\pi$ stacking interaction energies.[13] Formally of course this correlation applies only for

intermolecular and not (enforced) intramolecular interactions for which a BCP only implies local, and not overall stabilization.

In **1**, the presence of these two weak BCPs in turn results in location of four RCPs and hence of necessity, two CCPs. Boyd and co-workers[14] have recently shown how additional BCPs, originating in their case from a pair of F atoms in **4**, caused the ring surface to split into two as a result of the sterically induced helical twisting of the molecule. As a result, they suggested that a rare type of CCP bounded by only two RCPs is created, this being the only such example known at that time. The same phenomenon is now seen for **1**, although in this case the 2-fold helical twist, a property of the figure-eight lemniscular morphology, doubles this effect, resulting in two CCPs each bounded by two RCPs. These do not arise from ring completion due to F···F interactions but rather the rings created by the C···C π-stacking interactions. Boyd and co-workers[14] emphasized the importance of demonstrating the topological stability of identified critical points by showing that, e.g., any CCPs are appreciably distant from RCPs. Thus a separation of <0.2 Å between the points could indicate instability (and resulting self-annihilation) due to small geometrical changes such as those resulting from molecular vibrations. For **1**, the CCPs and the RCPs are separated by 1.24/1.14Å (cf. 0.6 Å reported for **4**), suggesting that **1** is a perfectly stable system to self-annihilation. The paths connecting the RCP 4 to the attractors (atoms) are shown ringed in purple (Figure 1); the equivalent symmetry-related paths are located for the other three RCPs. The paths connecting the CCP 5 include the six atoms (purple) and an additional three (orange).

4
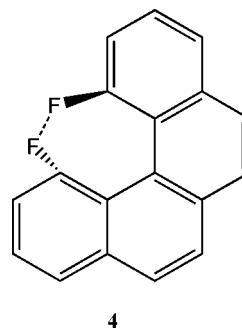
The electron density at the central RCP 3 (0.0166) is rather higher than that reported by Boyd (~0.01), the value for the four other RCPs (0.006) and the CCP (0.004) being somewhat smaller. Also confirmed is the reported[14] relative insensitivity of the analysis to the basis set and method. Thus the M05 DFT method,[15] which has recently been reported as being superior to the B3LYP procedure for predicting the bond length alternation in conjugated poly ynes (and hence presumably the electron density and associated correlation effects), gives almost identical values (Figure 1, for the common 6-31G(d) basis). Similar results are obtained employing B3LYP with the larger aug-cc-pvtz basis set. Further extending the basis set, such as including G or H functions, is not currently supported by the AIM2000 or AIMALL programs.[10] The signs and magnitudes of the Laplacian of the density, $\nabla^2\rho(r)$, which determines local concentrations and depletions in the electrons (~ +0.06 e Å^{-5} for point 3; +0.05 for point 2; +0.02 for point 5) and the energy density H(r) for point 2 (+0.003 H Å^{-3}) are similar to those

(10) (a) Biegler-König, F. W.; Schönbohm, J. *AIM2000* The program can be downloaded at http://www.aim2000.de/. (b) Keith, T. A. *AIMAll, Version 08.01.25*, 2008. URL: aim.tkgristmill.com.
(11) Kohout M. *DGrid, Version 4.3*, 2008.
(12) Humphrey, W.; Dalke, A.; Schulten, K. *J. Mol. Graphics* **1996**, *14*, 33–38.
(13) (a) Robertazzi, R.; Platts, J. A. *J. Phys. Chem. A* **2006**, *110*, 3992–4000. (b) Waller, M. P.; Robertazzi, A.; Platts, J. A.; Hbbs, D. E.; Williams, P. A. *J. Comput. Chem.* **2006**, *27*, 491–504. (c) Matta, C. F.; Castillo, N.; Boyd, R. J. *J. Phys. Chem. B* **2006**, *110*, 563–578.
(14) Castillo, N.; Matta, C. F.; Boyd, R. J. *Chem. Phys. Lett.* **2005**, *409*, 265–269.
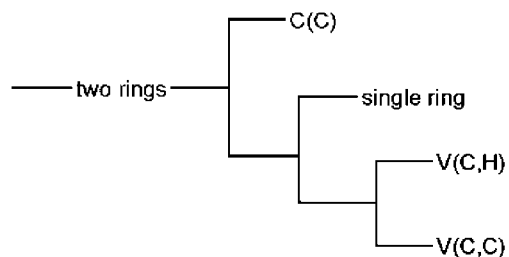(15) Zhao, Y.; Truhlar, D. G. *J. Phys. Chem. A* **2006**, *110*, 10478–10486.

FIGURE 2. Localization domain reduction tree diagram of **1**. The first separation is the core-valence separation. At the second bifurcation the valence domain splits (at the points where the AIM BCPs occur), and the structure becomes one single ring. Further reduction results in C,C and C,H valence basins.

reported[14] for the F···F BCP and RCP in **4** and point to a bond with ionic rather than shared character.

Analysis of the ELF for **1** reveals critical points of the same rank and signature and in similar positions to those located on the $\rho(r)$ surface by the AIM analysis.[16] No ELF basins exist at the positions of the BCPs at point 2 (Figure 1) in the ground state, which indicates that chemically no conventional C−C bond exists at this position.

The localization domain reduction tree (Figure 2) presents rather an unusual case. The first species in the tree is not, as might have been expected, a cyclic structure consisting of a single ring of 14 carbon atoms. It is in fact a structure with two rings due to a fusion of the carbon atoms at the lemniscular cross-over. The first bifurcation to occur is the core-valence separation. This is followed by separation of the two rings to form the single lemniscular loop. Web-enhanced Table 1 allows inspection of three isosurfaces describing this separation: the first showing the valence and core surfaces before separation of the two rings, the second at the point of separation, and the third after the two rings have separated. Of course this second splitting is not a formal bifurcation, since the two apparent valence domains that result are both part of the same domain. It is instructive to consider the tree in the way that Fuster and Silvi[17] considered those for weak, medium, and strong hydrogen bonds: "*In the weak hydrogen bond case, the reduction of the localization domain yields two domains in the first step, which can be partitioned afterward into valence and core domains. In contrast, for medium strength complexes, the core-valence separation is the first event which occurs during the reduction process and therefore the complex should be considered as a single molecular species.*"

Since in our case the core-valence separation is the first event to occur during the reduction process, the fused structure can be considered as a two-ringed species fused by weak C−C interactions (similar to the case of the medium-strength hydrogen bond analysis quoted above). This feature of the localization domain reduction tree supports the findings of the AIM analysis that there are medium/weak interactions between the central carbon atoms.

NICS Analysis of 1. In the previously reported analysis of **1**, the NICS(0) value at the ring centroid was reported as −18.2 ppm.[1] This corresponds exactly (due to symmetry) to critical point 3 (Figure 1) and indicates a strong diatropic ring current

at this ring centroid. This was interpreted[1] in terms of 4n+2 electron, double-twist (lemniscular) aromaticity. The AIM/ELF analysis now provides four further (and equivalent, by symmetry) RCPs, which sandwich two equivalent CCPs. The B3LYP/6-31G(d) NICS values (which might be designated NICS(rcp) or NICS(ccp)) at points 4 and 5 (Figure 1) are −7.9 and −8.6 ppm, respectively, indicative of a more modest but still clearly diatropic ring current in this region and hence suggestive of aromaticity (the NICS value at the centroid of benzene has a value of ∼−10 ppm).

Homoaromaticity. A chemical (as opposed to quantum topological) interpretation of the critical point analysis given in the previous section might be in terms of *homoaromaticity*, in which conventional cyclic π-conjugation is modified by insertion of a non-π-conjugating group such as CH_2.[18] Two different basic types have been proposed: the first is exemplified by the much studied homotropylium cation **5**, for which no BCP can be located in the C1−C7 region and which is hence termed as manifesting *no-bond homoaromaticity*; the other is a *bond-homoaromatic* type, of which **6** is characteristic.[18c] The presence
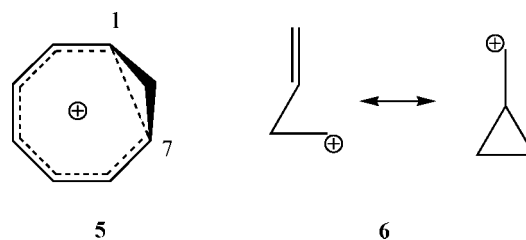
of four ring points 4 (Figure 1) deriving from two weak BCPs categorizes **1** as having a *bond-homoaromatic* 4n-electron half-twist Möbius ring system in each loop of the molecule and hence a diatropic ring current in each half. This has some analogy in the valence bond representations of naphthalene **7**. This can either have two equivalent 4n+2 6π-electron rings with a double bond in common or one 4n+2 10π-electron ring representing instead a [10]annulene with a single central bond. In the 14-electron system **1**, we have 4n 8π-electron diatropic ring currents resulting from a single half-twist Möbius-like circulation in each of the two equivalent ring paths in each "loop" of the figure eight. Superimposed is one single 4n+2 14π-electron ring current resulting from a double half-twist Möbius-like circulation in a 14π-electron single ring. No convincing candidates for *Homoaromatic* Möbius systems appear to have been hitherto proposed. Nor indeed has the unusual juxtaposition of diatropic ring currents resulting from single half-twisted cyclic conjugation following one selection rule (4n) coexisting with those generated by a double half-twist arrangement and following a different (4n+2) rule.

The implication of half-twist Möbius homoaromaticity in **1** leads to the question of whether other related examples might be identified. Schleyer and co-workers first reported[19] that the C_2-symmetric cation **8** exhibited Möbius aromaticity, as inferred by a modest (calculated) degree of bond length alternation around the ring, Δ_r, of 0.039 Å and a NICS value at the

---

(16) As a result of a slight variation in the topology of $\eta(r)$ relative to that of $\rho(r)$, nine RCPs are located instead of the five found for $\rho(r)$. The four RCPs corresponding to point 4 (Figure 1) are replaced by four pairs of RCPs. The remaining CPs required to fulfill the Poincaré−Hopf condition were not established.

(17) Fuster, F.; Silvi, B. *Theor. Chem. Acc.* **2000**, *104*, 13–21.

(18) (a) Childs, R. F. *Acc. Chem. Res.* **1984**, *17*, 347–352. (b) Cremer, D.; Kraka, E.; Slee, T. S.; Bader, R. F. W.; Lau, C. D. H.; Nguyen-Dang, T. T.; MacDougall, P. J. *J. Am. Chem. Soc.* **1983**, *105*, 5069–5075. (c) Lepetit, C.; Silvi, B.; Chauvin, R. *J. Phys. Chem. A* **2003**, *107*, 464–473. (d) Cremer, D.; Reichel, F.; Krafka, E. *J. Am. Chem. Soc.* **1991**, *113*, 9459–9466. (e) Geier, J. *J. Phys. Chem. A* **2006**, *110*, 9273–9281.

(19) Mauksch, M.; Gogonea, V.; Jiao, H.; Schleyer., P. v. R. *Angew. Chem., Int. Ed.* **1998**, *239*, 5–2397.
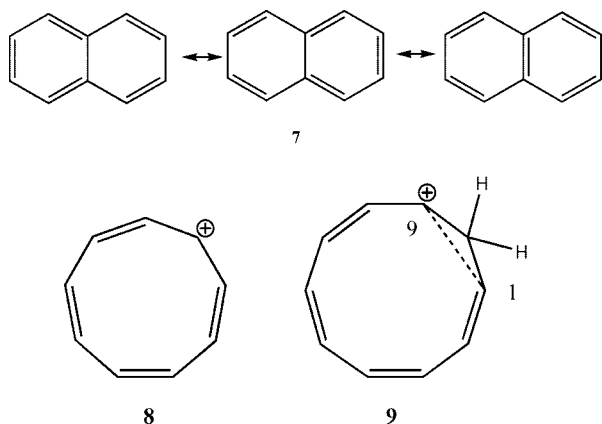
C-nuclear centroid indicative of diatropicity. The C_2-symmetric **9** is the methylene-bridged homoanalogue of **8**. Its C1−C9 separation is 1.69 Å (B3LYP/aug-cc-pVTZ), which is surprisingly short compared with the C1−C7 length in the homotropylium cation **5** (2.14 Å at the same level of theory) and only slightly longer than that for a true C−C single bond. AIM analysis (Figure 3) reveals no BCP in the C1−C9 region (likewise for **5**), showing that by the AIM criterion, **9** must be classified as a no-bond homoaromatic. The ELF localization domain reduction tree shows that by an ELF value of ∼0.71 all V(C,H) and V(C,C) all valence electron basins are separated (bifurcated). A V(C,C) basin between C1 and C9 is clearly visible, indicating (in contrast to the AIM analysis) the presence of a bond. However, whereas the other C−C basins vanish at ∼0.95, the V(C1,C9) all valence electron basin disappears at a much lower value (∼0.75, see Web-enhanced Table 1). This differing behavior supports the concept that the C1−C9 region is significantly different in character from (i.e., more delocalized than) the other C−C regions of the ring.

ELF bifurcation thresholds have been recently calibrated as measures of aromaticity.[20] For systems where a plane of symmetry allows σ/π separation, it was proposed that the ELF π-electron dissection $V(C,C)_\pi$ be used for this purpose, and values for typical aromatics range from 0.91 (benzene) to 0.64

(phenanthrene), dropping to a lower range of 0.11−0.35 for antiaromatics. While the C_2-symmetric **9** does not allow for a formal separation of the π-component, the four occupied MOs of π character are readily identified. The initial separation of the π-valence basins calculated using these MOs only in the ELF analysis commences at 0.495 in the C1−C9 region (Web-enhanced Table 1), but the rest of the π-ring bifurcates only at 0.80−0.88, which is certainly typical of the aromatic values noted previously for planar system.[20] The relatively low value for the π-bifurcation threshold of the C1−C9 basin, spanning of course a relatively long bond in this region (1.69 Å), suggests that any Möbius aromaticity scale based on this measure may not be entirely comparable with ones based on planar aromatics.

The NICS(rcp) value for **9** is −11.3 ppm, compared with −10.6 ppm calculated at the same level of theory (B3LYP/aug-cc-pVTZ) for **8**. The bond alternation, Δ_r, of 0.047 Å is also similar to that of **8**. These two indicators imply that the homoaromaticity in such a Möbius (C_2-symmetric) system may equal or even exceed that of its nonhomo analogue.

Reactivity. Other chemical inferences/connections can be made from the AIM critical point analysis. Vogel[21] demonstrated in 1982 how the 14π-electron bicyclic octalene **10** could be reduced to a dianion and then alkylated to the bicyclic **11**. The intermediate **11** could also arise from **1** by bond formation/cleavage in the region of one of the BCPs shown as point **2** (Figure 1). Species **11** was then observed to spontaneously undergo a 4n-electron electrocyclic ring opening, resulting in isolation of the monocyclic [14]annulene **12**. This was characterized as having the C_{2h}-symmetric conformation by crystallography.[20] It was previously recognized[1] that **12** (R = H) was indeed conformationally more stable than **1**. To explore these processes further, the transition states were located on the reaction path resulting from closing the weak interactions identified in **1** (Web-enhanced Table 1).
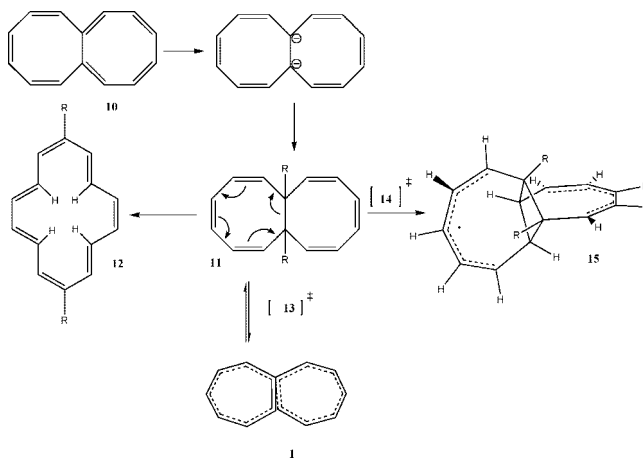
Transition state **13** corresponds to bond closure of **1** along one of the two BCPs (point **2**) and reveals only a small barrier separating **1** from the intermediate **11**, which is of similar stability to **1**. To achieve this closure in an allowed manner, the relative stereochemistry of the two groups shown as R in **11** must be specifically *cis*. As a result, both **11** and **13** are dissymmetric, each having C_2 symmetry. The point **13**, being
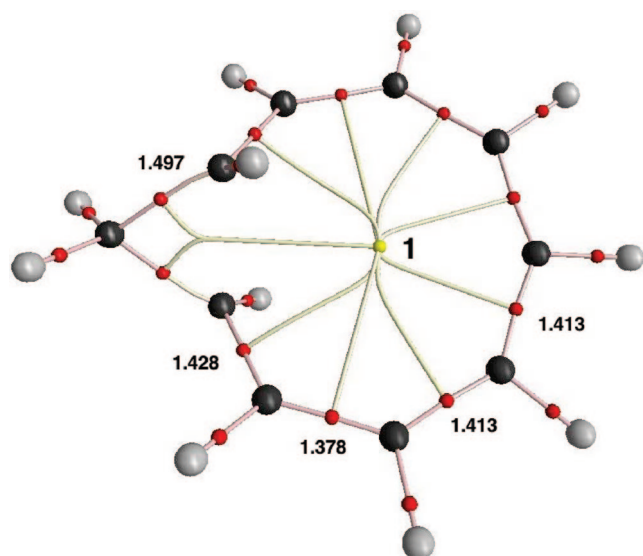
FIGURE 3. Paths connecting BCPs (3, −1, red) and the RCP (3, +1, yellow) for **9**. The $\rho(r)$ value for RCP 1 is 0.0036; the NICS value at 1 is −11.3 ppm. Bond lengths in angstroms.

(20) Santos, J. C.; Tiznado, W.; Contreras, R.; Fuentealba, P. *J. Chem. Phys.* **2004**, *120*, 1670–1673.

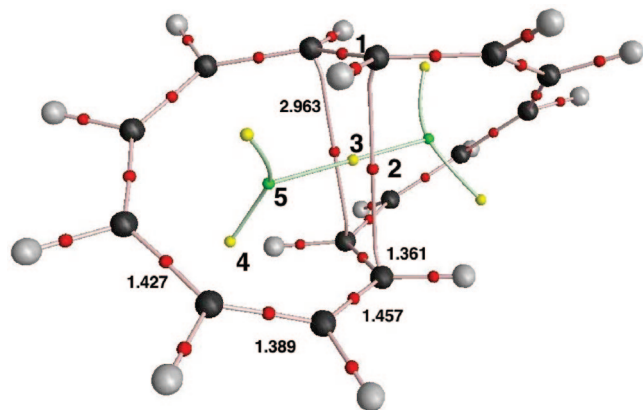(21) Vogel, E.; Engels, H. W.; Huber, W.; Lex, J.; Mullen, K. *J. Am. Chem. Soc.* **982**, *104*, 3729–3731.

FIGURE 4. Critical points for the dianion of **1** (color coding as for Figure 1). The $\rho(r)$ values for points 1–5 are 0.327, 0.012, 0.012, 0.045, and 0.034 au, respectively. The NICS values at ring centroid 3,4 and cage centroid 5 are 10.3, 7.7, and 8.6 ppm, indicative of a paratropic ring current. Bond lengths in angstroms.

classified as a 4n-electron electrocyclic thermal ring closure, can also be defined as a single half-twist Möbius aromatic transition state. It is in fact more subtle than that: the 2-fold symmetry means that the central forming bond is in fact common to two equivalent electrocyclic reactions; the arrows shown for **11** could equally well be drawn in the right-hand ring! This unusual situation, where two equally probable paths exist for the electronic rearrangement, was discussed at length,[22] citing **11** itself as an example. The analogy to the critical point analysis (Figure 1) now becomes more apparent. Each of the two CCPs 5 in **1** now represents the centroid for a nascent 4n-electron electrocyclization achieved by maintaining a C_2 axis of symmetry, and the Möbius *homoaromaticity* identified in **1** now becomes associated with Möbius transition state aromaticity in **13** (which in fact is only a minor perturbation to the structure of **1**). It is also noteworthy that **11** and **12** cannot be directly connected by a simple thermally allowed electrocyclic reaction, but that facile rotation about C=C bonds must also occur (as was suggested by Vogel).

A second (biradicaloid, S^2 before annihilation 0.6332, after 0.1991) transition state **14** now results from bond closure of the erstwhile second BCP in **1** to form a biradical **15**. This, having D_{2d} symmetry (when R = H), has a mirror plane, which in this case serves to act as the transition state for racemization of the dissymmetric **1** (or indeed equally dissymmetric **11**). The barrier is just sufficiently large to enable kinetic resolution of **1/11** (Web-enhanced Table 1).

4n-Electron Analogue of 1. Incrementing the π-electron count in **1** to the dianion results in a 4n count. This would be aromatic only as a single-half-twist system and would be inferred as non- or antiaromatic as a double-half-twist system. This manifests most obviously in the calculated geometry of the dianion, which exhibits Δ_r of 0.097Å, and strongly positive NICS values (Figure 4) at the RCPs and CCPs, indicative of paratropicity in all regions. In contrast, only a nonalternating geometry could be located for neutral **1**. Such lemniscular antiaromatics are unusual in not being able to undergo geometric buckling distortions to remove the antiaromaticity, as exemplified by, e.g., the tub-shape adopted by cyclo-octatetraene. Instead, the only available option for the system is to partition the C–C bonds into long and short lengths. Such bond
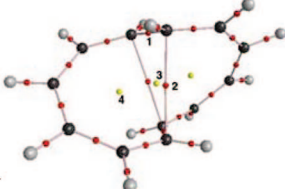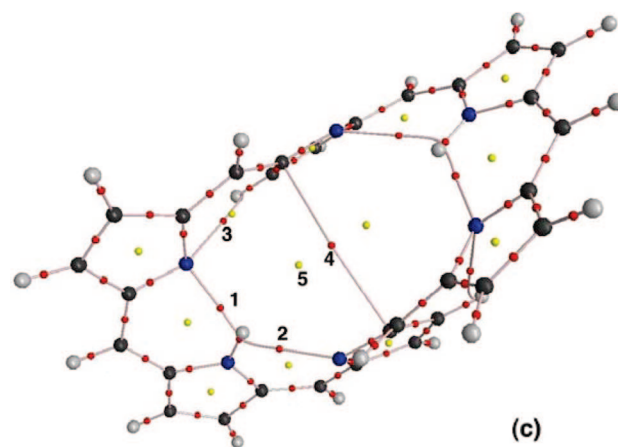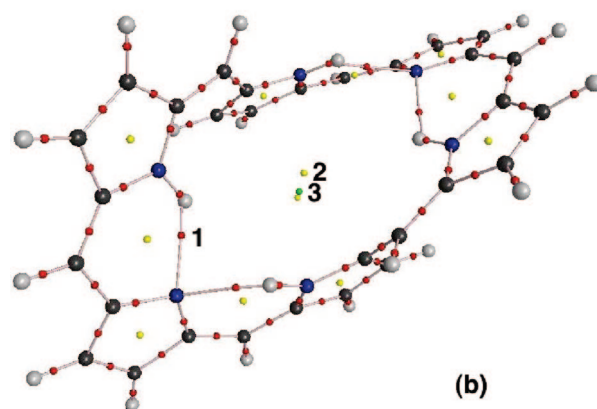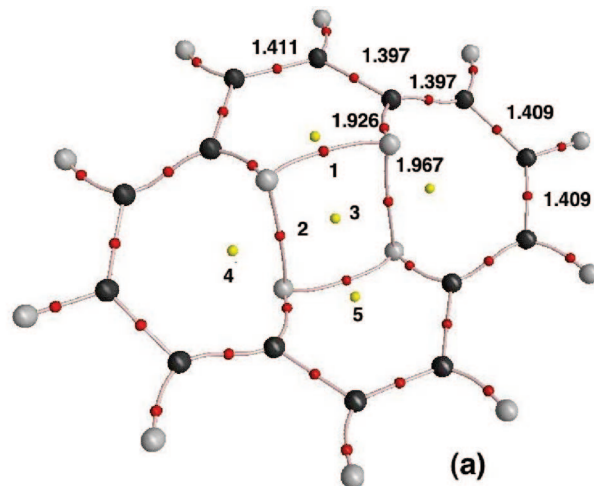
(22) Rzepa, H. S. *J. Chem. Educ.* **2007**, 1535–1540.
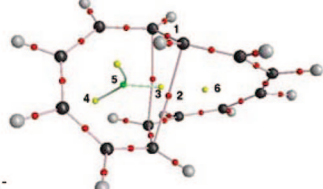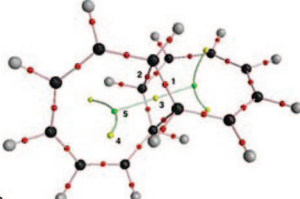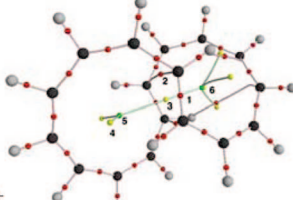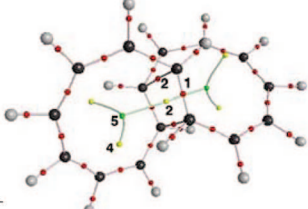
FIGURE 5. Critical points (color coding as for Figure 1) for (a) **12**. The $\rho(r)$ values for points 1–5 are 0.012, 0.007, 0.03, 0.004, and 0.012 au, respectively. Bond lengths in angstroms. (b) **2**. The $\rho(r)$ values for points 1–3 are 0.030, 0.0005, and 0.0002 au, respectively. (c) **3**. The $\rho(r)$ values for points 1–5 are 0.017, 0.028, 0.010, 0.0008, and 0.0007 au, respectively.

alternation is not merely speculation; it has been observed in the crystal structure of, e.g., [28]hexaphyrin[6] (see below).

The critical point analysis for the dianion nevertheless closely resembles that of **1** itself, the only significant difference being for point 2, where $\rho(r)$ is smaller. This results from the greater distance (2.96 Å) between the corresponding attractors compared to that in **1** (2.73 Å). Thus the (anti)aromaticity of the system has only a small effect on the outcome of the critical point analysis in this instance.

TABLE 2.   Critical Points and Associated Densities for [*n*]Annulenes as a Function of Ring Size

System	Critical point type	ρ-density
12-D_2^{2-}	Bond 1	0.299
	Bond 2	0.017
	Ring 3	0.016
	Ring 4	0.007
13-C_2^{-}	Bond 1	0.305
	Bond 2	0.018
	Ring 3	0.016
	Ring 4	0.009
	Cage 5	0.007
	Ring 6	0.004
14-D_2	Bond 1	0.309
	Bond 2	0.019
	Ring 3	0.017
	Ring 4	0.006
	Cage 5	0.004
15-C_2^{+}	Bond 1	0.330
	Bond 2	0.011
	Ring 3	0.010
	Ring 4	0.003
	Cage 5	0.002
	Cage 6	0.006
16-C_2^{2+}	Bond 1	0.312
	Bond 2	0.016
	Ring 3	0.014
	Ring 4	0.005
	Cage 5	0.003

Influence of Ring Size. The next issue addressed was whether the two weak BCPs associated with **1** were particular to it, or whether variation in ring size would change the outcome. Again, only minor variation in the BCPs was found when the annulene ring size is varied from 12 to 16 (while maintaining the 14-electron π-count, Table 2). Thus in the $[12]^{2-}$annulene, the two ring points 4 do not bifurcate into two, with no resulting cage point connecting them. For the $[13]^-$annulene, the two loops are of unequal sizes, and in the larger, the ring point 6 does not bifurcate, but it does do so in the smaller ring, resulting in cage point 5. The $[15]^+$annulene shows this bifurcation again for both rings, and the smaller ring manifests some additional bond/ring points associated with weak C–H$\cdots$C interactions. The $[16]^{2+}$ annulene has the same features as **1**. In all cases, the π–π stacking points are present as before, suggesting that this transannular interaction is not particularly sensitive to the ring size.

Other Systems. As noted previously,[1] **12** is a configurational isomer of **1** with the former being the more stable, with a speculation that the proximate H$\cdots$H interactions might have contributed to this stability. The four inward-facing hydrogens are indeed remarkably close, forming an almost perfect square with H$\cdots$H distances of 1.93 and 1.97 Å. A critical point analysis confirms four BCPs in this region (Figure 4a, points 1 and 2) with a RCP in the center (point 3), and four exocyclic RCPs (points 4 and 5). The $\rho(r)$ values however are relatively small, suggesting that local stabilization of the system by these effects is not great.

The hexaphyrins **2** and **3** (X = H, CF$_3$) contain a lemniscular cross-over, although the C–C separations are larger than in **1** (4.56 and 4.27 Å, respectively). This phyrin pair comprises one aromatic and one antiaromatic system.[23] The critical point analysis for aromatic **3** reveals obvious NH$\cdots$N intramolecular

hydrogen bonds (points 1 and 2, Figure 5), along with a less obvious CH$\cdots$N point (point 3). Of more relevance is the π–π stacking BCP (point 4) giving rise to one RCP in each loop of the lemniscate (point 5). The B3LYP/6-31G(d) NICS(rcp) value at each of these points is −10.9 ppm, indicative of diatropic and inferred homoaromaticity in each half of the lemniscate. The antiaromatic **2** in this case does not show any such C$\cdots$C stacking BCP, and the NICS(rcp) at the center of the lemniscate has the paratropic value of +10.5 ppm. An interesting recent observation by Schleyer and co-workers[24] implies that intramolecular π–π stacking of two *antiaromatic* rings, in which a close approach is enforced by a cyclophane-like scaffold, results their individual antiaromaticities combining to give a combined diatropicity (aromaticity). This behavior contrasts strongly with that of the aromatic **1** or **3**, in which a close self-approach gives rise instead to two homoaromatic regions.

Conclusions

Application of critical point analysis reveals the properties of cyclic lemniscular π-conjugated systems as exhibiting some unusual behavior. Not only is there an expected bond and ring path for the cycle as a whole, but individual bond and ring paths in each loop of the lemniscate can be interpreted chemically as indicating homoaromaticity or homoantiaromaticity, depending on the electron count. If the concept of Möbius homoaromaticity is applied to a cationic system such as **9**, it emerges as a particularly effective mode of conjugation; a prediction that may deserve experimental exploration.

(23) Rzepa, H. S. *Org. Lett.* **2008**, *10*, 949–952.

(24) Corminboeuf, C.; Schleyer, P. v. R.; Warner, P. *Org. Lett.* **2007**, *9*, 3263–3266.